

Supporting Information for:

**Analysis of the Radiation-Damage-Free X-ray Structure of
Photosystem II in Light of EXAFS and QM/MM Data**

Mikhail Askerka¹, David J. Vinyard¹, Jimin Wang², Gary W. Brudvig^{*,1},
Victor S. Batista^{*,1}

¹*Department of Chemistry, Yale University, New Haven, Connecticut 06520-8107,*

²*Department of Molecular Biophysics and Biochemistry, Yale University, New Haven, CT
06520-8114, United States*

Section I. EXAFS Calculation and Analysis.....2

Section II. Electron Density Maps Analysis.....4

Section III. References.....7

Section I. EXAFS Calculation and Analysis.

Calculation of the EXAFS

FEFF 8.30¹ combined with IFEFFIT² v.1.2.11d programs were used to compute the EXAFS spectra of the S₁ and S₀ models. Only the QM layers were taken into account for computing the EXAFS of the QM/MM optimized structures. For the current calculations, we considered all paths with lengths up to eight scattering legs and the extremely small contribution from hydrogen atoms was not considered. A value of 0.003 Å for the Debye–Waller factors was employed in all calculations. The energy (E) axis was converted into photoelectron wave vector (k) space by using the following transformation; $k = (2m_e/(h/2\pi)^2)(E - E_0)$ where m_e is the mass of the electron and h is Planck's constant. A value of $E_0 = 6540.0$ eV for the Fermi energy has been employed for the calculations involving the QM/MM model. A fractional cosine-square (Hanning) window with $\Delta k = 1$ was applied to the k^3 -weighted EXAFS data. The grid of k points, which are equally spaced at 0.05 \AA^{-1} , was then used for the Fourier transformation (FT) to R space. A k range of $4.2 - 16.6 \text{ \AA}^{-1}$ and the Hanning window for the FT for the isotropic EXAFS data was employed.

EXAFS Analysis

The EXAFS spectra simulated from the crystal structure data presented in both k -space (see main text) and reduced distance space (Figure S1) do not match the experimental spectrum nor do they match each other.

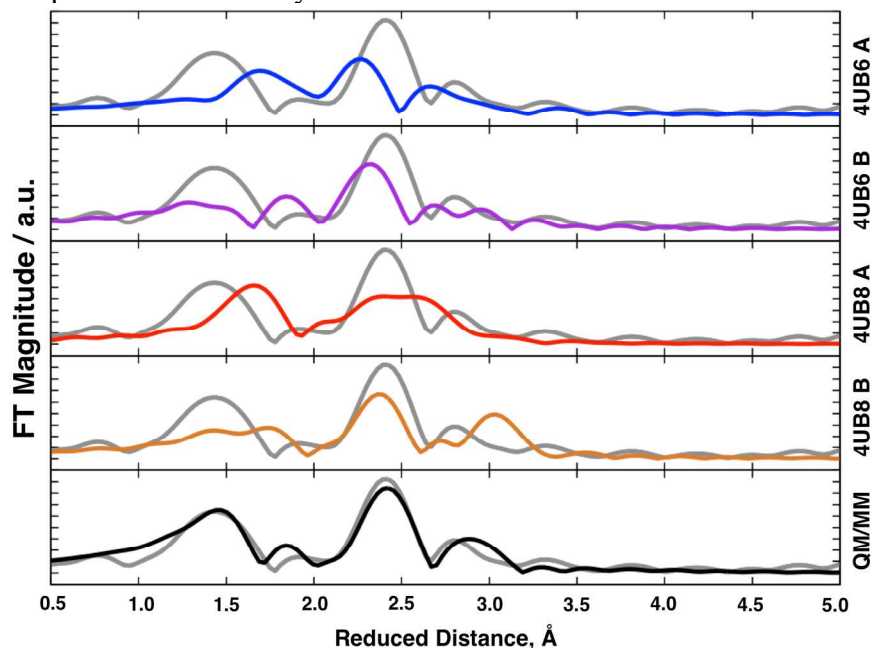


Figure S1. Fourier transforms of the EXAFS spectrum simulated from the 4UB6 monomer A (blue), monomer B (purple) and 4UB8 monomer A (red), monomer B (orange) crystal structures³ compared to the experimental⁴ S₁ spectrum (grey). The simulated EXAFS spectrum of our previously reported QM/MM structure⁵ for S₁ is shown in black for comparison.

The simulated metal-only extended range EXAFS spectra of the four OEC crystal structures and our QM/MM models of S_0 and S_1 show that the linear combinations of QM/MM metal-only EXAFS of S_0 and S_1 can be used to fit the EXAFS from the experimental crystal structures.

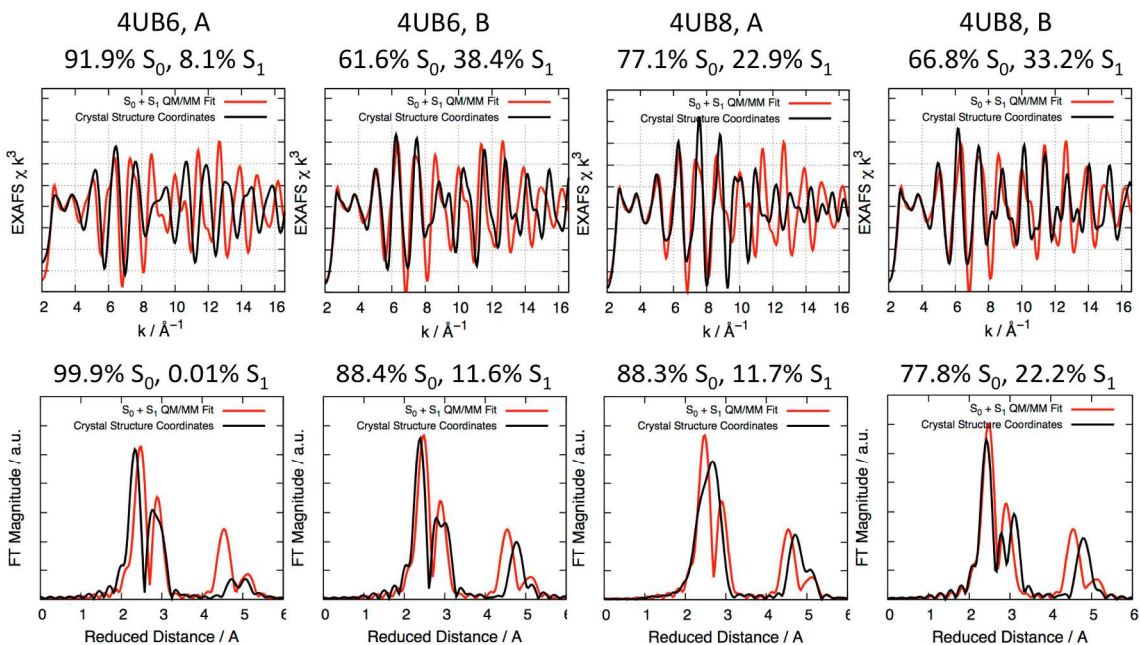


Figure S2. Simulated metal-only EXAFS spectra of the four OEC structures from reference³ were fit to linear combinations of QM/MM metal-only EXAFS of S_0 and S_1 .⁵ Fittings were performed on k -space data and Fourier transforms.

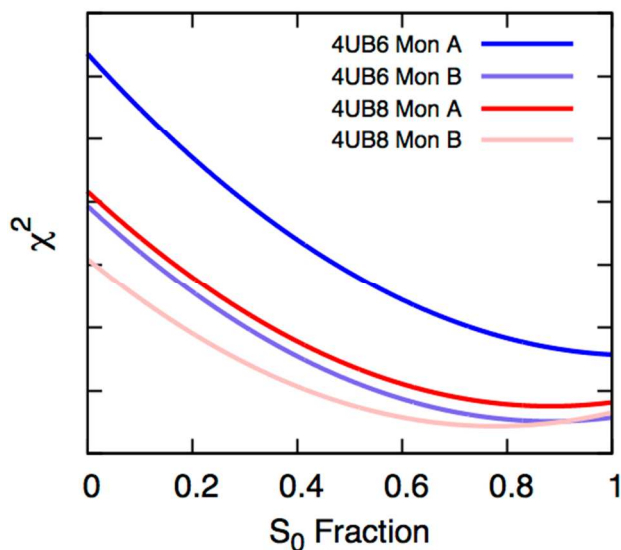


Figure S3. Precision of Fourier Transform fit profiles for data in Figure S2. χ^2 was calculated for each relative S_0 population. $[S_1] = 1 - [S_0]$.

Section II. Electron Density Maps Analysis.

The electron density maps were calculated using the observed amplitudes and calculated phases weighted with proper figure of merits deposited in the 3ARC entry at a nominal resolution of 1.9 Å. These maps show that peaks for water molecules bound to Ca and the peak for the O5 atom with relatively long lengths of coordination bonds are indeed well resolved in that structure. Two peaks for water molecules bound to Mn4 begin to be resolved. Small peaks for all remaining bridging small μ -oxygen atoms are completely unresolved from large peaks for Mn atoms at any contour levels.

A major finding in the two new structures (4UB8 and 4UB6) relative to the original structure (3ARC/3WU2) is that O5 has different coordination bond lengths to Mn atoms. Because the quality of 4UB8 structure is slightly better than that of 4UB6, the Mn3-O5 pair from monomer B of 4UB8 was placed on an axis for calculation of ideal error-free electron density functions using experimentally determined B-factors and interatomic distance between them, namely 22.14 Å² for Mn3 and 16.73 Å² for O5, and the distance of 2.38 Å (Fig. 2). Scattering factors of neutral Mn(0) and O(0) atoms were used for this calculation as were used for the original structure refinement. This calculation shows that when the contribution of the O5 atom is added to the Mn electron density function, the peak for the Mn atom is indeed shifted towards the O5 atom, and when contribution of the Mn atom is added to the O5 electron density function, the peak for O5 disappears, that is, the tail of the Mn electron density distribution is actually much higher than the peak density of O5 itself (Figure S4). The resolution of these atoms in the experimental maps would be even poorer when errors in experimental amplitudes and model-phases were taken into account given that there was a large disagreement R_{free} value of 22.5% between the observed and calculated amplitudes for 4UB8. Estimated coordinate errors for light-atom O atoms next to Mn inside the OEC of unknown geometry should be much larger than an overall error of protein atoms of known geometry with similar size of atoms, the latter which was reported to be 0.27 Å for the 4UB8 entry. Finally, the Fourier truncation ripple effect of Mn results in extra density for O, making O appear to have more electron density than it should have (Fig. S4F). This may also explain why O5 has a much smaller B-factor than those of the surrounding Mn atoms.

If B-factors for the Mn-O pair are reduced to 15, 10, 5, and 0 Å², the peaks for the two atoms are then gradually resolved, particularly when the B-factor is below 10 Å². However, when their B-factors are reduced without a corresponding increase of nominal resolution, ripple effects of Fourier truncation also gradually increase. The first peaks of the ripple are at 2.1 Å, approximately coincident with the Mn3-O5 coordination bond length. If the large Mn atom is replaced with the smaller Mg atom with the fixed interatomic distance of 2.32 Å, peaks for atoms of the Mg-O pair in the electron density map calculated at a nominal resolution of 1.95 Å now begin to show a diatomic feature. Thus, the resolution problem of the Mn and O peaks is specific to the disparity in their number of electrons. Thus, the resolution of protein molecule atoms of equal size in the nominal resolution is actually better than for oxygen atoms next to big Mn atoms.

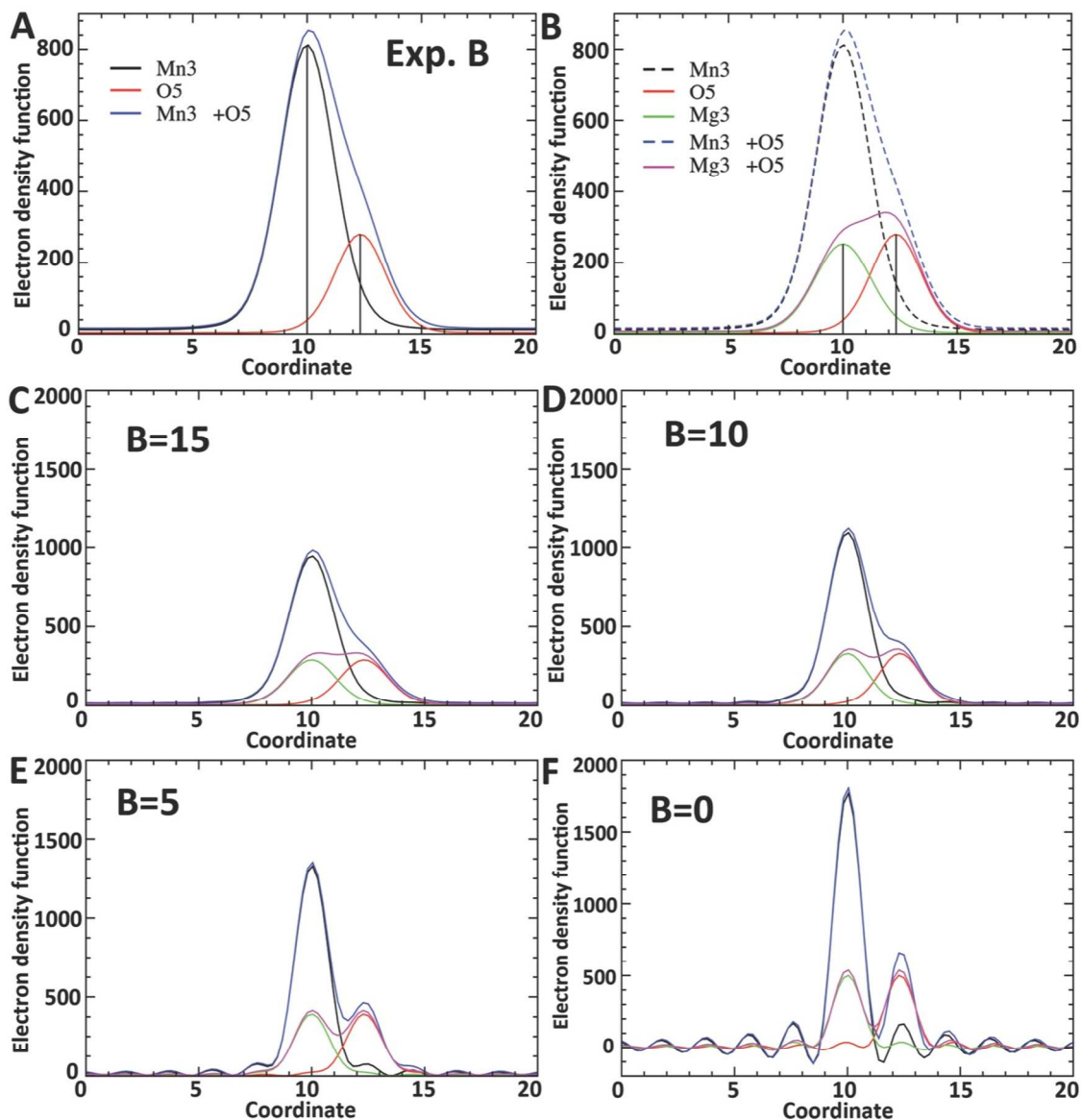


Figure S4. Resolution of atoms at a nominal resolution of 1.9 Å. (A) Using experimentally determined B-factors for Mn3 ($B=22.14 \text{ \AA}^2$) and O5 ($B=16.75 \text{ \AA}^2$) and their interatomic distance (2.32 Å) in the OEC of monomer B in 4UB8. Idealized electron density functions (maps) for Mn (black) and O (red) atoms as well as the combined electron density functions (blue) in an arbitrary unit without volume factor calibration. The contribution of the Mn atom completely overshadows the O atom, making it invisible. The peak positions in the omitted maps for the omitted O atoms in a model represent their positions in the model when Mn positions are not refined or are fixed in place during the refinement. (B) If Mn were Mg, the effect of overshadowing is reduced where di-atomic features begin to emerge. (C-F) When data were sharpened or the B-factors for the two atoms are reduced to 15, 10, 5, and 0 Å², these two atoms are gradually resolved. However, if the nominal resolution does not increase accordingly and remains at 1.95 Å for the 4UB8 structure, the Fourier truncation ripple effects begin to increase. The first peaks of heavy Mn ripple effects (which are actually the first sphere in a three-dimensional structure, and the first ring in a two-dimensional structure) are approximately coincided with the location of O5.

This confirms that peaks for atoms of the Mn3-O5 pair are not resolved at a nominal resolution of 1.95 Å in a one-dimensional structure. The resolution in the three-dimensional structures (Figure 2B, main text) will of course be better than the one-dimensional structure because errors in two orthogonal directions introduced by overlapping peaks should be smaller than the error along the bonding axis. It is important to note that the difference between Mn(0) used in structure refinement and the actual Mn(IV) in the OEC is 4 electrons, which can affect the accuracy of the refined B-factors, and thus the slope of the electron density function of Mn near its tails of the distribution.

Overall, this calculation shows that effects of incorrectly positioned O atoms in structure refinement are relatively small on the placements of Mn atoms, and hence the positions of Mn atoms can very accurately be determined at this resolution. However, any small errors in Mn positions can dramatically affect the placements of O atoms, and hence the positions of O atoms may not have been accurately refined at this resolution given relatively high R-factors of about 20% for these structures. The Mn-O situation is very different from a Mg-O pair, the latter of which is more easily determined at this nominal resolution because of the approximately equal size of the two atoms.

Section III. References.

- [1] Ankudinov, A. L., Bouldin, C. E., Rehr, J. J., Sims, J., and Hung, H. (2002) *Phys Rev B* 65, 104107.
- [2] Newville, M. (2001) *J Synchrotron Radiat* 8, 322-324.
- [3] Suga, M., Akita, F., Hirata, K., Ueno, G., Murakami, H., Nakajima, Y., Shimizu, T., Yamashita, K., Yamamoto, M., Ago, H., and Shen, J.-R. (2014) *Nature* 517, 99-103.
- [4] Haumann, M., Muller, C., Liebisch, P., Iuzzolino, L., Dittmer, J., Grabolle, M., Neisius, T., Meyer-Klaucke, W., and Dau, H. (2005) *Biochemistry* 44, 1894-1908.
- [5] Pal, R., Negre, C. F. A., Vogt, L., Pokhrel, R., Ertem, M. Z., Brudvig, G. W., and Batista, V. S. (2013) *Biochemistry* 52, 7703-7706.